

ChemComm

Accepted Manuscript



This is an *Accepted Manuscript*, which has been through the Royal Society of Chemistry peer review process and has been accepted for publication.

Accepted Manuscripts are published online shortly after acceptance, before technical editing, formatting and proof reading. Using this free service, authors can make their results available to the community, in citable form, before we publish the edited article. We will replace this *Accepted Manuscript* with the edited and formatted *Advance Article* as soon as it is available.

You can find more information about *Accepted Manuscripts* in the [Information for Authors](#).

Please note that technical editing may introduce minor changes to the text and/or graphics, which may alter content. The journal's standard [Terms & Conditions](#) and the [Ethical guidelines](#) still apply. In no event shall the Royal Society of Chemistry be held responsible for any errors or omissions in this *Accepted Manuscript* or any consequences arising from the use of any information it contains.

All-In-One Azides: Empowered Click Reaction for *in vivo* Labeling and Imaging of Biomolecules

Received 00th January 20xx,
Accepted 00th January 20xx

Yaning Su,^{a, c, †} Li Li,^{b, c, †} Haibin Wang,^c Xiaochen Wang^c and Zhiyuan Zhang^{c, d, *}

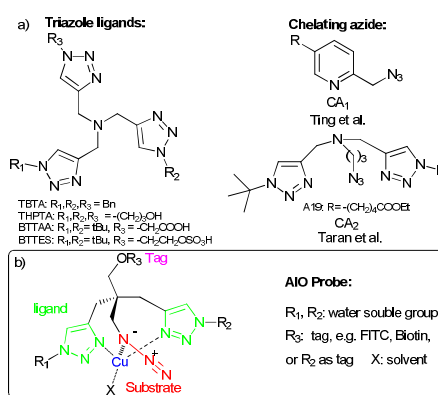
DOI: 10.1039/x0xx00000x

www.rsc.org/

We designed and synthesized all-in-one (AIO) reactive azide reagents for bioorthogonal reactions with highly efficient Cu(I) ligand moieties, an azido group, and functional tags for imaging or purification. The AIO reagents displayed fast and efficient click ligation and can be applied in a wide range of *in vivo* systems.

The past two decades have witnessed the development and widespread application of bioorthogonal reactions for selectively labeling biomolecules without using genetic modifications.¹ Among all the bioorthogonal reactions, ligand assisted copper(I) catalyzed azide-alkyne cycloaddition (CuAAC) reactions are the most broadly applied one.² To date, CuAAC has been widely applied in the labeling and imaging of proteins,³ glycans,⁴ nucleic acids⁵ and other macromolecules⁶ both *in vitro* and *in vivo*. To guarantee the reaction speed and the overall efficiency of CuAAC reactions *in vivo*, excessive amounts of Cu(I) complex (copper sources, ligands, and sodium ascorbate) are typically required, which results in copper (I) mediated cellular toxicity that casts a shadow on their further application in living systems.^{1a,7}

One strategy to improve the biocompatibility of CuAAC reactions is to modify the structure and compatibility of the Cu(I) ligand to improve ligation kinetics and efficiency and decrease copper loading. Ligands with enhanced water solubility such as THPTA,⁷ BTAA⁸, and BTES³ (Scheme 1) have been developed and been shown to accelerate the CuAAC reaction significantly and to act as ROS scavengers to decrease Cu(I)-induced cell toxicity. A more effective strategy is developing highly reactive azides by combining Cu(I) chelating moieties and the azide component in one molecule to raise the effective copper concentration. This strategy was first exploited by Ting et al., who combined a copper chelating pyridine group into the substrate azide skeleton (Scheme 1,



Scheme 1 (a) Structure of classic triazole ligands and chelating azides. (b) Structure features of the All-In-One reagents.

CA₁).⁹ This chelating azide showed much faster kinetics than standard azides, and had efficient performance in bioorthogonal labeling with the assistance of THPTA as a ligand. Recently, the Taran group combined the triazole ring, a stronger Cu(I) chelating moiety into the azide reagent (Scheme 1, CA₂).¹⁰ Their system showed even faster kinetics than ligand catalyzed CuAAC reactions and was effective in labeling and imaging tubulin without additional ligands.

The structure of CA₂ was derived from triazole ligands for CuAAC, with two triazole rings linked to the nitrogen atom at the center of the skeleton. It is speculated that the fast kinetics is resulted from the intramolecular chelation pattern that enhances the electrophilicity of azido group and formation of the metallacycle intermediate.¹⁰ With the third arm of the nitrogen atom left for an azido group acting as a war-head for further bioorthogonal coupling, tags for detection or purification for application in biological systems would have to be added to the triazole rings. However, since modifications at this position are necessary to improve the reactivity and solubility as shown in THPTA and BTES, this tag linkage might undermine the properties of the tagged reactive azides.

In order to preserve the positions for compound property adjustment and to provide a more flexible scaffold for tag conjugation, herein, we report the design and synthesis of a

^a College of Life Sciences, Beijing Normal University, Beijing 100875, China

^b School of Life Sciences, Peking University, Beijing 100871, China

^c National Institute of Biological Sciences (NIBS), Beijing 102206, China. E-mail: zhangzhiyuan@nibs.ac.cn

^d Collaborative Innovation Center for Cancer Medicine, Beijing, China, 102206

† These authors contributed equally to this work.

unique version of reactive azides, the All-In-One (AIO) copper chelating azide reagents with a tetrahedron carbon atom at the core of the structural skeleton (Scheme 2). By placing a tetrahedron carbon atom at the center, a total of four arms can be utilized to fulfill different aspirations. With two arms linked by triazole rings and the third arm as an azido group, the fourth arm remains free for various choices for tag fragments. This leaves positions R_1 and R_2 (Scheme 2) free for the convenient adjustment of reactivity and biocompatibility of AIO reagents.

We first evaluated the kinetics and overall performance of AIO reagent **1** in a pure chemistry system. (See ESI for full synthesis details). A model reaction, in which AIO reagent **1** reacts with a coumarin derivative to form a fluorescent product **5** (Fig. 1a), was selected for the kinetic study; the formation of product was measured via its fluorescence.¹⁵ (Fig. S1, S2, S3) The model reaction was carried out in the presence of different concentrations of Cu(I) (0.25 to 4 equivalent). The fluorescence intensity of **5** was measured every 6 seconds during a total time course of 5 minutes. The yield and time course of the reaction was compared with TBTA, the typical CuAAC ligand, BTTES and THPTA, a water soluble ligand, and most

importantly, with A19 (Scheme 1, CA₂), the chelating reactive azide Taran reported. The kinetic study results indicate that AIO reagent **1** is extremely active, yielding product **5** at 60% within 90 seconds (Fig. 1b). The chelating azide A19 showed similar kinetics but a little lower yields (48%), and other control reactions catalyzed by ligands only had yields of no higher than 13%, at 5 min (Fig. 1b).

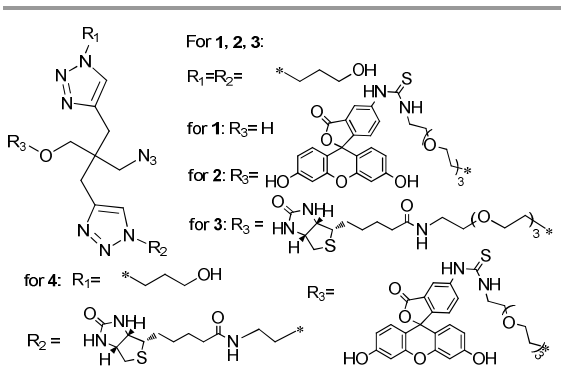
The observed rate constant k_{obs} of **1** was calculated. When the CuSO₄ level was under 1 equivalent, the reaction rate depends on Cu(I) concentration, increasing from 28 M⁻¹ · s⁻¹ at 0.25 equivalent of Cu to 121 M⁻¹ · s⁻¹ at 1 equivalent of Cu (Table S1, Fig. S4, Fig. S6). However, the reaction rate was highly similar when the CuSO₄ level was in the range of 1~4 equivalents. Under the same reaction condition (with 1 equivalent of Cu(I)), k_{obs} of reactions catalyzed by other ligands were also tested and compared. The k_{obs} (121 M⁻¹ · s⁻¹) of AIO reagent **1** is much higher than that of TBTA (0.39 M⁻¹ · s⁻¹), THPTA (0.99 M⁻¹ · s⁻¹), BTTES (1.23 M⁻¹ · s⁻¹), and slightly higher than A19 (82 M⁻¹ · s⁻¹ Table S1, Fig. S4).

Since the differences in the amounts of CuSO₄ were observed to affect the rate constant, we next investigated the order of Cu in this reaction. By plotting $\ln[k_{obs}]$ versus $\ln[CuSO_4]$, we discovered that the order of Cu appeared to differ depending on its loading. The order was determined to be 0.99 under conditions of insufficient CuSO₄, while with excessive amounts of CuSO₄, the rate order was 0.08, which indicates that the reaction rate is independent on the CuSO₄ concentration when the Cu supply is more than one equivalent (Fig. S5).

It was proposed that copper chelating azides facilitates the formation of metallacycle intermediate in the rate-determining step, leading to the fast kinetics.^{10,12} To test if AIO reagents have similar reaction mechanism, we measured the association constant (K_a) of AIO reagent **1**, **A19** and their corresponding products (**5** and **25**) with Cu(I). Chelating azides and their products all have similar affinity with Cu(I), which are about 20-fold higher than that of non-chelating azide with premixed TBTA and Cu(I) complex (Fig. S8).⁵ These results provided evidence that chelating azides coordinate to copper in a more efficient way than standard azides, which might in turn promote the metallacycle intermediate formation.

Recently, halide inhibition of CuAAC reaction has been reported.^{7,13} We set out to evaluate the effect of halides on AIO reagents assisted CuAAC reaction. The model reaction was carried out using 1 equivalent of Cu(I), accompanied by the addition of 1 equivalent or 100 equivalent of NaX (X=Cl, Br, I). The real-time detection of the reaction course (Fig. S10, S11, Table S2) indicated that only minor inhibition was seen under the condition of 100 equivalent of sodium iodide, while no obvious inhibitions were seen on both the yield and reaction rate under the other halide conditions. The good halide tolerance property of AIO reagents provided a guarantee for applications in biological systems.

It has been reported that triazole ligands such as THPTA,⁷ BTTES³ and BTAA⁸ all have protective effect towards Cu(I) induced toxicity. Due to the structure similarity, we investigated whether AIO reagent **1** has protective effects for cell viability when they were co-incubated with Cu(I). Cells



Scheme 2 Structure of AIO probes.

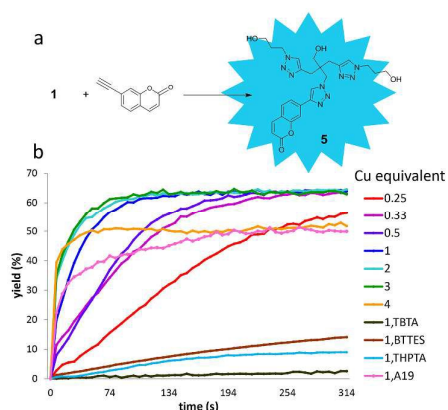


Fig.1 (a) Model reaction for kinetic measurements. (b) Time course under different CuSO₄ equivalents. For AIO reagent **1** and A19, reactions were performed with 10 μM **1** or A19, 100 μM 7-ethynylcoumarin, 100 mM sodium ascorbate and different equivalence of CuSO₄ accordingly. Control reactions with triazole ligands were performed with 50 μM 2-azidoethanal, 50 μM CuSO₄, 500 μM 7-ethynylcoumarin, 100 mM sodium ascorbate. All reactions are carried out in DMF: H₂O 1:1 solution.

incubated with Cu(I) alone for 4 hours had an extremely high incidence of cell death (survival rate is less than 5%), even when the Cu(I) concentration was as low as 20 μ M. The presence of AIO reagent **1**, however, showed an obvious protective effect, increasing the rate of cell survival to more than 90% at even 100 μ M Cu(I) (Fig. S12). Complexes composed of Cu(I) and A19/THPTA/TBTA/BTTES also showed protective effects, all raising the cell survival rate to more than 40% at 100 μ M Cu(I) treatment.

Encouraged by the results of the evaluation of the AIO reagent properties, we next evaluated the utility of the AIO click reaction in live cells. For this purpose, we synthesized FITC or biotin tagged reagents **2** and **3** (Scheme 2, See ESI for full synthesis details). Jurkat cells were cultured in the presence of peracetylated N-(4-pentynoyl)mannosamine ($Ac_4ManNAI$), a modified biosynthesis precursor of alkynyl sialic acid, so that the bioorthogonal alkyne group can be assembled on cell surface glycoproteins through a biosynthesis procedure (Fig. S13).^{3,4b}

The reactivity of FITC-tagged AIO reagent **2** was investigated initially. The alkyne labeled cells were treated with a mixture of AIO **2** (100 μ M) and $CuSO_4$ (100 μ M), together with 10 mM sodium L-ascorbate for 1 hour. A clear and strong green fluorescence in the FITC channel was observed in the $Ac_4ManNAI$ treated cells, and this merged well with the red fluorescence from cell membrane stained with Dil (Fig. 2a, S14, S15). In the control sample lacking $Ac_4ManNAI$ treatment, the green fluorescence was hardly visible (Fig. 2a, S14, S15), indicating that AIO reagent **2** can efficiently label membrane proteins on the surface of living cells. Next, the performance of AIO reagent **3** (Scheme 2) was evaluated in the biotin pull-down process. Alkyne labeled Jurkat cells were collected and lysed. This was followed with the AIO click reaction, biotin affinity pull down experiments, and Western blotting. As indicated, the Western blots had clear bands in the $Ac_4ManNAI$ treated sample but not in the control sample (Fig. 2b).

In addition to the mono-tag AIO reagents **2** and **3**, we also synthesized a bi-tag AIO reagent **4** (Scheme 2), which has both biotin and FITC moieties. This bi-functional AIO reagent can be

used for imaging and affinity purification at the same time. We tested the application of **4** using the aforementioned alkyne modified Jurkat cells. After affinity purification with the biotin tag, the isolated portion was examined for both the biotin and FITC tags; apparent and sufficient glycoprotein imaging and biotin labeling is shown (Fig. 2c). This bi-functional AIO reagent can be further applied in activity-based protein profilings to isolate labeled protein via fluorescent signals from SDS gel after biotin-streptavidin enrichment, which could simplify the whole procedure and at the same time lower the background signals.

To explore the further potential of this AIO labeling, we tested its application in chemical genetics, a recently developed research field that includes active small molecule-based target identification starting from phenotype screening.¹⁴ Human epidermal growth factor receptor 2 (HER2) and its covalent binding inhibitor (compound **6**, Canertinib analogue with EC_{50} =20 nM for Ba/F3-HER2) (Fig. 3a) were chosen for our investigation of activity based targeting of specific protein (Fig. S16).¹⁵ Treatment of HER2/H878Y-transformed BA/F3 cells with compound **6** localized the bioorthogonal alkyne group on HER2 through covalent binding of the probe with the intracellular kinase domain of HER2.^{15b} Cells were then incubated with the fluorescence AIO reagent **2**/ $CuSO_4$ /sodium ascorbate complex. In order to confirm the localization of the FITC labeling, cells were fixed and immunostained with HER2 antibody. The fluorescence of FITC was mainly concentrated at the cell membrane region, and the FITC fluorescence coincided well with the red fluorescence of the HER2 immunostaining (Fig. 3b, S17), indicating that AIO reagent **2** successfully penetrated into cells and labeled the protein-bound probe with the imaging tag.

The affinity pull-down assay showed a similar performance of probe **3** in targeting applications in complex systems. Cell lysates obtained from compound **6** preincubated cells were treated with AIO reagent **3** for the labeling of the biotin tag. Following streptavidin affinity pull-down, the HER2 signal was clearly present in the Western blot (Fig. 3c) compared with the control group, which had not been treated with compound **6**.

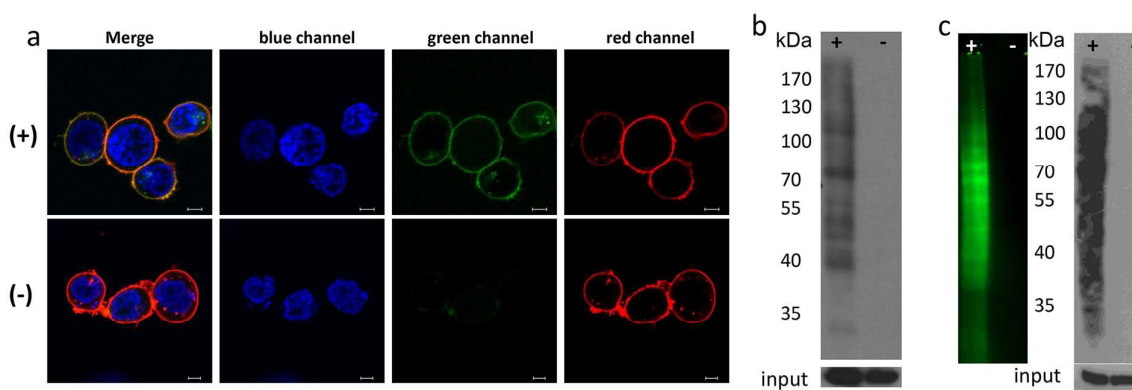


Fig. 2 (a) Confocal microscopy images of probe **2** labeling on the surface of live Jurkat cells. (blue channel: Hoechst; green channel: FITC; red channel: Dil. Scale bar: 5 μ m) (b) Western blot analysis for biotin tag after probe **3** labeling on the Jurkat cell proteome. (c) In-gel fluorescence and biotin Western blotting for the detection of labeling efficiency of bifunctional probe **4**. (+): cells cultured with 100 μ M $Ac_4ManNAI$; (-): cells cultured without $Ac_4ManNAI$. For all imaging and labelling, 100 μ M AIO reagents/ $Cu(I)$ complex was used.

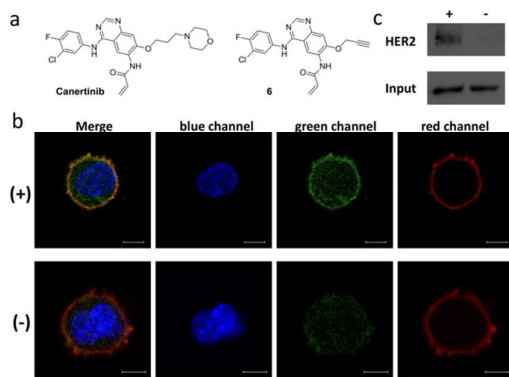


Fig. 3 (a) Structures of canertinib and its alkyne analogue 6. (b) Confocal microscopy images of probe 2 labeled HER2/H878Y-transformed BA/F3 cells. (blue channel: Hoechst; green channel: FITC; red channel: anti-HER2 immunostaining). Scale bar: 5 μm . (c) Western blot of HER2 after affinity pulldown by probe 3 in the HER2-transformed BA/F3 proteome. (+): cells treated with 10 μM compound 6 for 3h; (-): cells treated with DMSO. For all imaging and labelling, 100 μM AIO reagents/Cu(I) complex was used after compound 6 was washed away.

These results indicated that AIO labeling system can be used in activity based protein profiling (ABPP) applications for target identification, target localization and functional study with active small molecules.

After we successfully labeled cell surface glycoproteins and HER2 kinase *in vivo*, we focused our efforts on labeling and imaging in a living organism, *C. elegans*. *C. elegans* is an excellent model organism for studies of glycan dynamics in development, disease, and normal physiological processes.¹⁶

We cultured *C. elegans* larvae on nematode growth medium (NGM)-agar plates without (untreated, “-”) or with 5 mM Ac₄GalNAI (treated, “+”) for at least two generations. The mixed-stage Ac₄GalNAI worms were soaked in 100 μM AIO reagent 2/Cu(I) for 40 min, washed softly, and recovered for 4 h on NGM plates prior to imaging. In young adult hermaphrodites, GalNAI-specific labeling was clearly observed in pharynx and tail regions (Fig. 4b,e,f), in accordance with previous reports,²⁶ while no specific staining was observed in control worms (Fig. 4a,c,d). Similar staining patterns were observed in worms that were treated with much lower concentrations of AIO reagent or Ac₄GalNAI (250 μM) (Fig. S18), highlighting the high labeling efficiency of AIO reagent 2.

To conclude, AIO reagents displayed efficient ligation and had excellent catalytic kinetics and obvious cellular protective effect against Cu(I)-induced toxicity. We successfully

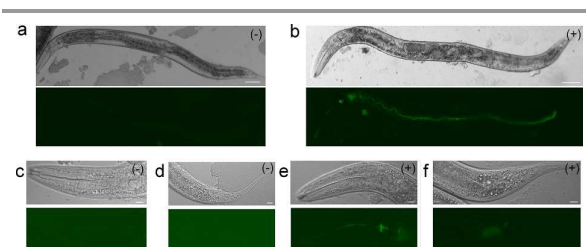


Fig. 4 (a-b) Confocal imaging of live *C. elegans* young adult hermaphrodites after probe 2 labelling. Scale bar: 50 μm . (c-f) Higher magnification images of the pharynx (c, e) and tail region (d, f). Scale bar: 10 μm . (+: Ac₄GalNAI-cultured worms; -: normally cultured worms.) For labelling and imaging, 100 μM AIO reagents/Cu(I) complex was used.

demonstrated the application of AIO reagents for bioorthogonal ligation at several levels of biological organization, from the *in vivo* labeling of cell membrane glycoproteins and the specific targeting of a protein with an irreversible inhibitor beyond to live imaging applications with *C. elegans*. All of these properties offer a strong endorsement for suitability of the AIO reagents to be applied in experiments to address challenging and relevant biological questions.

This work is supported by National High Technology Project 973 (2011CB504300). We thank Mr Fanqi Zeng, Mr Pengfei Liu and Mr Dong Wang for their organic synthetic work, imaging services of Imaging Facility (NIBS) and Institute of Biophysics, Chinese Academy of Sciences for ITC instrument.

Notes and references

- For discussion of the proposed reaction mechanism, see Supporting Information (page S22-25)
- (a) E. M. Sletten and C. R. Bertozzi, *Angew. Chem., Int. Ed.*, 2009, **48**, 6974; (b) K. Lang and J. W. Chin, *Chem. Biol.*, 2014, **9**, 16.
- J. E. Moses and A. D. Moorhouse, *Chem. Soc. Rev.*, 2007, **36**, 1249.
- D. Soriano del Amo, W. Wang, H. Jiang, C. Besanceney, A. C. Yan, M. Levy, Y. Liu, F. L. Marlow and P. Wu, *J. Am. Chem. Soc.*, 2010, **132**, 16893.
- (a) T. L. Hsu, S. R. Hanson, K. Kishikawa, S.-K. Wang, M. Sawa and C.-H. Wong, *Proc. Natl. Acad. Sci. U. S. A.*, 2007, **104**, 2614; (b) P. V. Chang, X. Chen, C. Smyrniotis, A. Xenakis, T. Hu, C. R. Bertozzi and P. Wu, *Angew. Chem. Int. Ed.*, 2009, **48**, 4030.
- (a) A. Salic and T. J. Mitchison, *Proc. Natl. Acad. Sci. U. S. A.*, 2008, **105**, 2415; (b) C. Y. Jao and A. Salic, *Proc. Natl. Acad. Sci. U. S. A.*, 2008, **105**, 15779.
- C. Y. Jao, M. Roth, R. Welti and A. Salic, *Proc. Natl. Acad. Sci. U. S. A.*, 2009, **106**, 15332.
- V. Hong, S. I. Presolski, C. Ma and M. G. Finn, *Angew. Chem., Int. Ed.*, 2009, **48**, 9879.
- C. Besanceney-Webler, H. Jiang, T. Zheng, L. Feng, D. Soriano del Amo, W. Wang, L. M. Klivansky, F. L. Marlow, Y. Liu and P. Wu, *Angew. Chem., Int. Ed.*, 2011, **50**, 8051.
- C. Uttamapinant, A. Tangpeerachaikul, S. Grecian, S. Clarke, U. Singh, P. Slade, K. R. Gee and A. Y. Ting, *Angew. Chem., Int. Ed.*, 2012, **24**, 5852.
- V. Bevilacqua, M. King, M. Chaumontet, M. Nothisen, S. Gabillet, D. Buisson, C. Puente, A. Wagner and F. Taran, *Angew. Chem., Int. Ed.*, 2014, **53**, 5872.
- Z. Zhou and C. J. Fahrni, *J. Am. Chem. Soc.*, 2004, **126**, 8862.
- (a) G.-C. Kuang, H. A. Michaels, J. T. Simmons, R. J. Clark and L. Zhu, *J. Org. Chem.*, 2010, **75**, 6540; (b) W. S. Brotherton, H. A. Michaels, J. T. Simmons, R. J. Clark, N. S. Dalal and L. Zhu, *Org. Lett.*, 2009, **11**, 4954.
- (a) R. M. Moorman, M. B. Collier, B. H. Frohock, M. D. Womble and J. M. Chalker, *Org. Biomol. Chem.*, 2015, **13**, 1974; (b) S. Lal and S. Díez-González, *J. Org. Chem.*, 2011, **76**, 2367; (c) V. O. Rodionov, S. I. Presolski, D. Díaz Díaz, V. V. Fokin and M. G. Finn, *J. Am. Chem. Soc.*, 2007, **129**, 12705.
- B. R. Stockwell, *Nat. Rev. Genet.*, 2000, **1**, 116.
- (a) J. B. Smaill, G. W. Rewcastle, J. A. Loo, K. D. Greis, O. H. Chan, E. L. Reyner, E. Lipka, H. H. Showalter, P. W. Vincent and W. L. Elliott, *J. Med. Chem.*, 2000, **43**, 1380; (b) B. R. Lanning, L. R. Whitby, M. M. Dix, J. Douhan, A. M. Gilbert, E. C. Hett, T. O. Johnson, C. Joslyn, J. C. Kath and S. Niessen, *Nat. Chem. Bio.*, 2014, **10**, 760.
- (a) S. T. Laughlin and C. R. Bertozzi, *Chem. Bio.*, 2009, **4**, 1068; (b) H.-Y. Hwang, S. K. Olson, J. D. Esko and H. R. Horvitz, *Nature*, 2003, **423**, 439.